The specific heat and upper critical field $B_{c2}(T)$ of amorphous Cu_xSn_{100-x} - electronic and vibrational excitations

1996 J. Phys.: Condens. Matter 8 6857

(http://iopscience.iop.org/0953-8984/8/37/008)

J. Phys.: Condens. Matter **8** (1996) 6857–6872. Printed in the UK

The specific heat and upper critical field $B_{c2}(T)$ of amorphous Cu_xSn_{100-x}—electronic and vibrational excitations

M Sohn and F Baumann

Physikalisches Institut, Universität Karlsruhe (TH), 76128 Karlsruhe, Germany

Received 13 June 1996, in final form 29 July 1996

Abstract. The specific heat C of amorphous Cu_xSn_{100-x} films ($10 \leqslant x \leqslant 70$) was investigated between 0.3 K and 7 K in the superconducting state as well as in the normal state using a modified AC method. The analysis of the data allows one to determine the electronic density of states at the Fermi energy $D(E_F)$, the density of states of low-energy excitations n_0 and the Debye temperature Θ_D. The concentration dependence of $D(E_F)$ shows a pronounced minimum at $x = 60$ at.% in comparison to the free-electron model, in agreement with specific heat and UPS measurements and theoretical calculations published recently. The specific heat of the low-energy excitations is of the same order of magnitude as data available from the literature, and shows a linear temperature dependence. Θ_D increases with copper concentration and the values agree with those published recently.

In addition, the critical magnetic field $B_{c2}(T)$ of the same films was measured. The analysis of these data which should be valid for strongly disordered superconductors yields values of $D(E_F)$ which are about 20% higher than those determined by specific heat measurements. Arguments are given as to why values taken from critical field measurements might be too high.

Finally, the specific heat of an amorphous $Au_{70}Sn_{30}$ film was measured. $D(E_F)$ was found to be 30% below the free-electron model value, in contrast to results published previously by Rieger and Baumann who found $D(E_F)$ to be in accordance with the free-electron model.

1. Introduction

The close relationship between atomic structure and electronic properties of amorphous metals has attracted great interest in recent years. Numerous theoretical investigations came to the conclusion that the electronic density of states (DOS) should be lowered in those regions of reciprocal space where the structure function has a maximum [1–3]. Of special interest is the situation where the structure-induced minimum in the DOS is located at the Fermi energy E_F [4].

First evidence for a minimum in the DOS at E_F was found for amorphous Au_xSn_{100-x} films (a-Au_xSn_{100-x}) and similar alloys [4, 5] often called amorphous Hume-Rothery phases (AHR) [4] using photoelectron spectroscopy. UPS spectra show a decrease of the DOS towards E_F. Because the d electrons of the noble metals are located well below E_F, AHR alloys are very suitable for this type of investigation and their electronic properties can be compared with those derived from the free-electron model (FEM). Deviations from the FEM for these alloys can be attributed to a structural influence. Besides, photoelectron spectroscopy deviations were found in the Hall effect of AHR alloys [4] and in the electronic specific heat of a-Cu_xSn_{100-x} [6]. They are most pronounced for high noble-metal content.

0953-8984/96/376857+16$19.50

In the case of a-$Mg_{70}Zn_{30}$ a minimum of the DOS was predicted for theoretical reasons and validated by UPS measurements [7]. However, in specific heat measurements no deviations from the FEM could be found [8].

Recently the DOS of a-Au_xSn_{100-x} was determined using both specific heat and critical field measurements [9]. The authors found the concentration dependence of the DOS to be in agreement with the FEM. This result is very surprising because a decrease of up to about 50% was expected according to UPS measurements [4].

The purpose of this investigation is twofold. Firstly, we extend measurements of the specific heat C of a-Cu_xSn_{100-x} in zero field [6] to magnetic fields higher than the critical field $B_{c2}(T)$. This allows us to measure the electronic contribution to C in the normal state at temperatures below the superconducting transition temperature T_c and to achieve therefore a higher accuracy. In addition to the specific heat the upper critical field $B_{c2}(T)$ of the same sample is measured. For superconductors with an extremely short mean free path, e.g. amorphous metals, $D(E_F)$ can be calculated from $B_{c2}(T)$. Hence a second method is available to determine $D(E_F)$, which is completely independent of specific heat results.

Secondly, with a refined experimental method we wanted to verify specific heat measurements on a-Au_xSn_{100-x} published by Rieger and Baumann [9] in order to test whether $D(E_F)$ for these alloys shows a FEM-like behaviour or a structure-induced minimum. For the experiments discussed below, a phase-sensitive AC method for specific heat measurements proposed by Velichkov [10] was established and carefully tested [11]. Its high sensitivity gives us confidence that we could treat the problems mentioned above successfully and that it was reasonable to measure the specific heat of a-Cu_xSn_{100-x} and a-Au_xSn_{100-x} to some extent for the second time.

2. Some experimental details

The amorphous films were obtained by flash evaporation of small portions of the alloy onto a sapphire substrate held at low temperatures. Because the films transform from the amorphous into the crystalline state at temperatures well below room temperature, the whole experiment had to be performed *in situ*. To prevent a large increase of temperature during the condensation process, the substrate for the specific heat measurements was thermally well coupled to a liquid helium bath. Whereas most methods for measuring the specific heat require a thermally isolated sample, an AC-heating method is suitable and often used in measuring the specific heat of quench-condensed films [9, 12].

In this investigation most of the measurements were carried out with a modified AC-heating method proposed by Velichkov [10]. With this method the sensitivity in measuring the heat capacity of thin films could be raised by at least one order of magnitude compared to that for the method used earlier [6, 9], to about 10 pJ K^{-1} at 0.3 K. Details of this phase-sensitive method are published elsewhere [11]. In order to test the experimental set-up and the measuring method, the specific heat of a crystalline gallium sample was measured [11] and compared with data taken from the literature [13]. On the basis of this calibration the absolute values of heat capacities in this work are accurate to about 5% in the normal state, and to about 20% in the superconducting state due to the lower heat capacity.

The heat capacity of the films was determined in zero field and in a perpendicular field larger than the critical value to force the films to the normal state. The measurements were carried out between 0.3 K and 7 K. Beside the heat capacity the electrical resistance of a simultaneously condensed film was measured using a standard DC four-probe method. This allows us to determine $B_{c2}(T)$ and the electrical resistivity $\rho(T)$. The mass of the film was determined with a total inaccuracy of 5 μg from the mass difference of the calorimeter

before and after condensation of the sample using a precision balance. Typical masses were between 0.3 and 1 mg for the sample and between 60 and 80 mg for the whole calorimeter.

3. Results

The electrical resistivity ρ and its concentration dependence, the temperature of the transition to superconductivity T_c, and the crystallization temperature T_k measured during annealing were found to be in good agreement with the data known from the literature [4, 6, 14–19]. and will not be shown here. Only the measurements of the specific heat $C(T)$ and the upper critical field $B_{c2}(T)$ which allows one to determine the electronic density of states at E_F in the case of amorphous superconductors are presented.

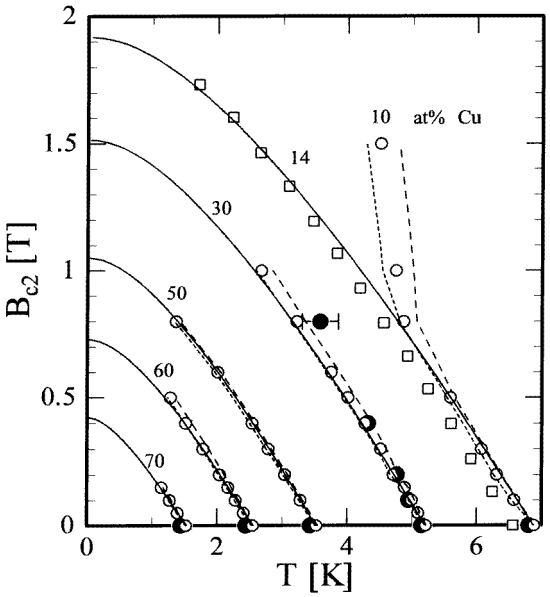

Figure 1. Temperature dependences of the upper critical field $B_{c2}(T)$ of a-Cu_xSn_{100-x}: (●) heat capacity measurements—all other symbols are for resistance measurements; (○) 50% of residual resistance; (- - - -) 10% of residual resistance, (– – –) 90% of residual resistance; (□) from Bergmann [21].

3.1. The upper critical magnetic field

For amorphous superconducting films such as a-Cu_xSn_{100-x}, the perpendicular critical magnetic field $B_{c\perp}(T)$ is equal to the upper critical magnetic field $B_{c2}(T)$ [20]. A plot of $B_{c2}(T)$ is shown in figure 1. The numbers next to the curves indicate the copper content x. In order to characterize the width of the transition, dashed lines mark the fields at 10% and 90% of the residual resistance while the circles indicate the midpoint of the resistive transition. In the case of a-$Cu_{30}Sn_{70}$, critical fields were not only determined by resistance measurements but also by specific heat measurements. For comparison, some data taken from the literature are also shown.

The full lines are fits to the WHH theory [21, 22] which obviously describes the data very well, except that for the film a-$Cu_{10}Sn_{90}$. The crystallization temperature of this film is $T_k = 40$ K which is the lowest of the crystallization temperatures for all of the samples under investigation. For this reason this film is probably inhomogeneous and may exist in at least two different superconducting phases. At higher fields not used in this investigation Bergmann found slightly higher values of $B_{c2}(T)$ in comparison to WHH theory [21].

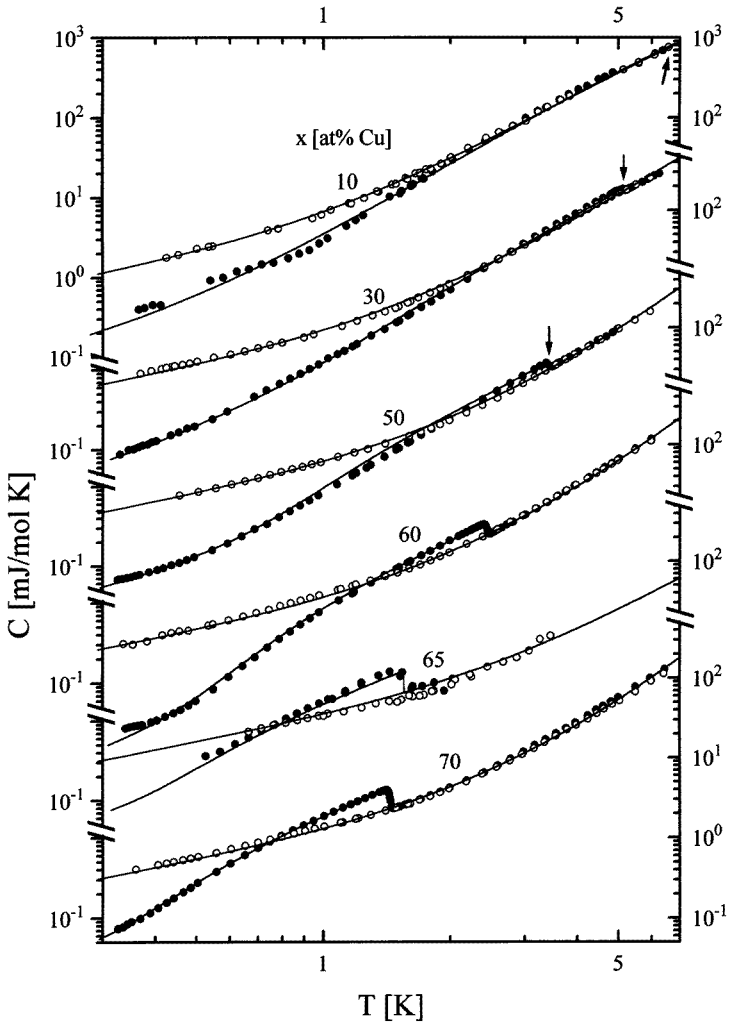

Figure 2. Temperature dependences of the specific heat $C(T)$ of a-Cu_xSn_{100-x} with logarithmic scales. Note the shifted scales of the vertical axis. The arrows point at the transition to superconductivity at T_c; (●) without magnetic field; (○) with $B > B_{c2}(T)$. The numbers next to the curves give the Cu contents of the films.

For amorphous metals like a-Cu_xSn_{100-x} the slope of $B_{c2}(T)$ at T_c is given by [23]

$$\left.\frac{dB_{c2}}{dT}\right|_{T=T_c} = \eta\frac{4k_B e}{\pi}\rho D^{\star}(E_F) \qquad (1)$$

with Boltzmann's constant k_B, the elementary charge e, electrical resistivity ρ and the enhanced density of states $D^\star(E_F)$ at the Fermi energy. The constant η is equal to one within a few per cent [24]. In the case of amorphous superconductors equation (1) provides an additional possibility for determining $D^\star(E_F)$ and will therefore be a valuable complement to specific heat measurements. In the case of amorphous metals like a-Cu_xSn_{100-x} the enhancement is caused by the electron–phonon interaction. $D^\star(E_F)$ is connected to the bare or 'undressed' density of states $D(E_F)$ by [25]

$$D(E_F) = D^\star(E_F)/(1+\lambda) \tag{2}$$

with λ describing the electron–phonon coupling.

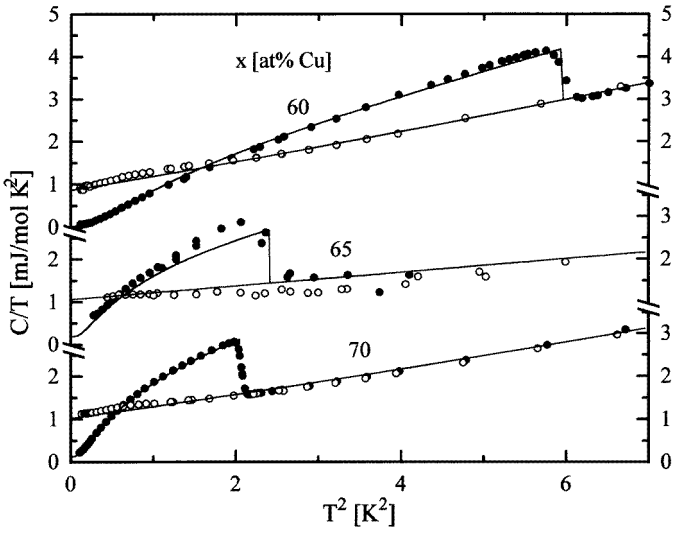

Figure 3. C/T of a-Cu_xSn_{100-x} as functions of T^2. Note the shifted scales of the vertical axes; (●) without magnetic field; (○) with $B > B_{c2}(T)$. The numbers next to the curves give the Cu contents of the films.

3.2. Specific heat

The specific heat $C(T)$ of the a-Cu_xSn_{100-x} films measured in this investigation is shown in figure 2. Full and open circles represent the data with and without an applied magnetic field $B > B_{c2}$, respectively. The curves are least-squares fits to the data and will be explained later. With increasing copper content the temperature T_c of the transition to superconductivity decreases and the jump in $C(T)$ at T_c becomes more and more pronounced as the total specific heat decreases at lower temperatures. At the same time the specific heat at high temperatures decreases with increasing copper content. This trend reflects an increasing Debye temperature of these alloys with increasing x. The data in figure 2 were taken with the phase-sensitive method [11] except in the case of the a-$Cu_{65}Sn_{35}$ film which was measured with the technique from references [9, 26]. The great gain in resolution of the new method in comparison to the old one can be seen immediately. This is also visible in figure 3 in which some of the curves are replotted in the usual representation: C/T as a function of T^2. Again the curves represent fits to the data.

In order to analyse the data we describe the specific heat $C(T)$ as the sum of a vibrational part $C_{\mathrm{vib}}(T)$ and an electronic part $C_{\mathrm{e}}^{\mathrm{n}}(T)$ in the normal state and $C_{\mathrm{e}}^{\mathrm{s}}(T)$ in the superconducting state. In the normal state

$$C_{\mathrm{e}}^{\mathrm{n}}(T) = \gamma T \tag{3}$$

and

$$\gamma = \frac{1}{3}\pi^2 k_{\mathrm{B}}^2 D^{\star}(E_{\mathrm{F}}). \tag{4}$$

In the superconducting state we evaluate $C_{\mathrm{e}}^{\mathrm{s}}(T)$ in a first approximation according to the BCS theory for weak electron–phonon coupling using tabulated values [27] which are used for the fits shown in figures 2 and 3. Deviations from this behaviour in the strong-coupling films with small copper content can be described by equation (8) as will be discussed below. For the electron–phonon coupling parameter λ see figure 9 of this work, later.

The vibrational term $C_{\mathrm{vib}}(T)$ is obtained by summing the contributions of the phonons $C_{\mathrm{L}}(T)$ and the low-energy excitations $C_{\mathrm{LEE}}(T)$. According to the two-level-tunnelling model [28] the contribution of the LEE is

$$C_{\mathrm{LEE}}(T) = aT = \frac{\pi^2}{6} k_{\mathrm{B}}^2 n_0 T \tag{5}$$

where n_0 represents the density of the two-level systems which is assumed to be constant. The phonon part $C_{\mathrm{L}}(T)$ is approximated by [29]

$$C_{\mathrm{L}} = \beta T^3 + \delta T^5 \tag{6}$$

neglecting higher-order terms. The coefficient β and the Debye temperature Θ_{D} are connected by

$$\beta = \frac{12}{5}\pi^4 R \Theta_{\mathrm{D}}^{-3}. \tag{7}$$

The term δT^5 and those of higher order which get important at higher temperatures reflect the phonon dispersion.

It has to be stressed that the four parameters γ, a, β, δ are determined by fitting simultaneously the specific heat data in the normal and the superconducting state, of course with the requirement of equal entropy for $T = T_{\mathrm{c}}$. Table 1 gives the values of these parameters as well as the concentration x, and the mole number n of the films, the annealing temperature T_{a}, the crystallization temperature T_{k}, the transition temperature to superconductivity T_{c} and the residual resistivity ρ. The fitting curves are shown as thin lines in figures 2 and 3.

In order to give the reader some insight into the quality of the evaluation of the data just mentioned, we show the different contributions to the heat capacity for the two limiting examples. Figure 4 gives the analysis in the case of a-$Cu_{70}Sn_{30}$ which has the lowest electron–phonon coupling of the films investigated and its $C_{\mathrm{e}}^{\mathrm{s}}(T)$ can be described by the BCS theory quite well. Figure 5 shows the evaluation in the case of a-$Cu_{30}Sn_{70}$ which is a strong-coupling superconductor. In both figures the solid line indicates the phonon part C_{L} while the filled circles give the specific heat in zero field $C(B = 0)$ reduced by substracting C_{L}; this is named ΔC below. The methods of evaluation of the data in the two cases are slightly different.

In the case of a-$Cu_{70}Sn_{30}$ (figure 4) the contribution $C_{\mathrm{e}}^{\mathrm{s}}(T)$ is calculated according to the BCS theory as mentioned above, using T_{c} and γ from table 1. The values of C_{LEE} shown as triangles are then calculated by subtraction of $C_{\mathrm{e}}^{\mathrm{s}}(T)$ from the data and fitted to equation (5). The self-consistency of this analysis can be shown by two tests. Firstly, we calculate $C_{\mathrm{e}}^{\mathrm{s}}(T)$

Table 1. Properties of a-Cu_xSn_{100-x} samples investigated together with the parameters from the fit of the measured specific heat to equations (3), (5), and (6).

x (at.%)	n (μmol)	T_a (K)	γ (mJ mol^{-1} K^{-2})	a (mJ mol^{-1} K^{-2})	β (mJ mol^{-1} K^{-4})	δ (μJ mol^{-1} K^{-6})	T_c (K)	T_k (K)	ρ ($\mu\Omega$ cm)
0[a]	—	—	1.77	—	0.2504	—	3.72	—	—
10[b]	2.642	a.q.	3.165	0.458	3.078	−12	6.8	40	41.6
30	4.122	a.q.	2.011	0.144	1.063	4.9	5.15	—	54.5
30	4.122	90	1.891	0.148	0.886	7.3	5.05	189	54.1
50	9.164	a.q.	1.444	0.137	0.529	7.6	3.43	—	67.0
60	8.178	a.q.	0.850	0.046	0.319	6.1	2.44	—	78.5
60	8.178	150	0.917	—	0.159	8.6	2.27	257	76.9
65	4.575	a.q.	0.873	—	0.158	—	1.55	296	—
70	10.039	a.q.	0.903	0.135	0.266	5.0	1.44	—	89.4
70	10.039	310[c]	0.739	0.199	0.046	7.0	0.85	310	82.0
100[a]	—	—	0.695	—	0.0476	—	—	—	—

[a] Mean of the values from different authors [29].
[b] This sample was not completely homogeneous.
[c] Annealing was interrupted by quenching of the sample during the crystallization process.

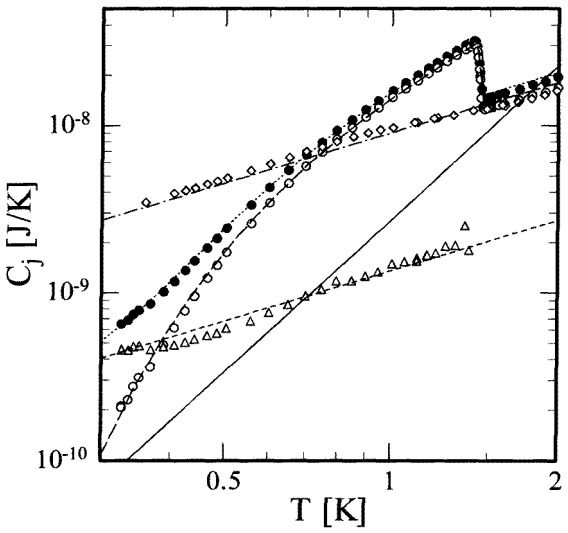

Figure 4. Temperature dependences of the different contributions C_j to $C(T)$ of the weak-coupling a-$Cu_{70}Sn_{30}$. The solid line gives C_L; ● represents $\Delta C = C(B = 0) - C_L$; (△) C_{LEE}; (○) C_e^s; (◇) C_e^n. In addition the fitting curves for the different contributions are shown.

(open circles) as the difference between ΔC (full circles) and the fit to C_{LEE} (dashed line) and compare it to the earlier fit to BCS theory (broken line). Secondly, we compare the values of $C_e^n(T)$ (shown as diamonds) obtained from $C(B > B_{c2})$ by subtracting both C_L and C_{LEE} to those calculated according to equation (3) (chain line).

In the case of the strong-coupling a-$Cu_{30}Sn_{70}$, we assume a linear temperature dependence of C_{LEE} and obtain this contribution by fitting ΔC (full circles) for $T < 1$ K to equation (5) (dashed line). $C_e^s(T)$ (open circles) is then calculated from ΔC by subtracting

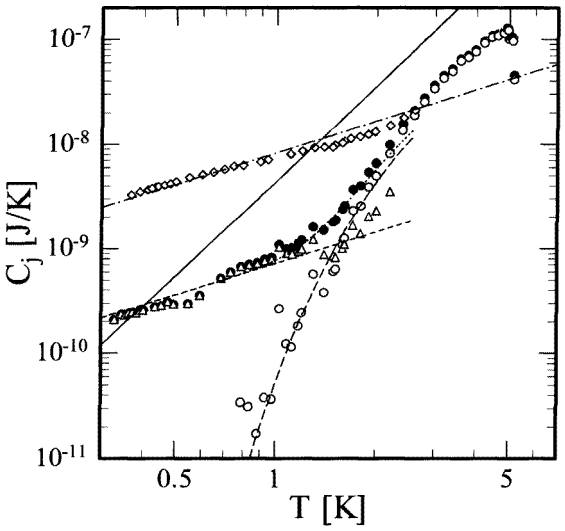

Figure 5. Temperature dependences of the different contributions C_j to the specific heat $C(T)$ of the strong-coupling a-$Cu_{30}Sn_{70}$. The solid line gives C_L; ● represents $\Delta C = C(B = 0) - C_L$; (△) C_{LEE}; (○) C_e^s; (◊) C_e^n. In addition the fitting curves for the different contributions are shown.

C_{LEE} and fitted to [30]

$$\frac{C_e^s(T)}{\gamma T_c} = a' e^{-bT_c/T} \tag{8}$$

which is valid for $2.5 \leqslant T_c/T \leqslant 6$ (broken line) yielding $a' = 8.4$ and $b = 1.71$. The self-consistency of this analysis is checked by comparing C_{LEE} calculated from ΔC by subtracting the fit to equation (8) (triangles) to the original fit (dashed line) and by comparing the values of $C_e^n(T)$ (shown as diamonds) obtained from $C(B > B_{c2})$ by subtracting both C_L and C_{LEE} to those calculated according to equation (3) (chain line). It is possible to determine the energy gap $\Delta(T = 0)$ in the excitation spectrum of a-$Cu_{30}Sn_{70}$ in the superconducting state from the fitting parameter b. In the weak-coupling limit the BCS theory gives $a' = 8.5$ and $b = 1.44$ corresponding to $2\Delta(0)/(k_B T_c) = 3.52$. From $b = 1.71$ we get $2\Delta(0)/(k_B T_c) = 4.19$ in agreement with tunnelling measurements [19] which give 4.28 for a-$Cu_{22}Sn_{78}$ and 3.98 for a-$Cu_{41}Sn_{59}$.

Whereas non-linear temperature dependencies of C_{LEE} are discussed for a-Zr alloys in the literature [31], the present investigation does not support a non-linear temperature dependence of C_{LEE} for a-Cu_xSn_{100-x}. It has to be stressed that in the present analysis of the data the fits to C_e^n, C_e^s and C_{LEE} are optimized consistently and that a non-linear temperature dependence of C_{LEE} causes deviations in C_e^n and C_e^s at the same time.

4. Discussion

In the analysis of our specific heat data we neglected contributions which may stem from nuclear quadrupole interaction, from Zeeman splitting or from electrons in normal-conducting regions in inhomogeneous samples. The validity of these assumptions should be discussed first.

X-ray diffraction measurements on quenched a-Cu_xSn_{100-x} films with $5 \leqslant x \leqslant 20$ [32] and electron diffraction measurements on a-Cu_xSn_{100-x} and a-Au_xSn_{100-x} [14, 15] give no indication of any inhomogeneity. On the other hand due to the proximity effect precipitations in these alloys embedded in a superconducting matrix have to be at least 10 nm thick in order to become normally conducting [33]. In addition, annealing of the quenched films changed the electrical resistivity and the transition temperature T_c only very little as long as the crystallization process was not initiated. The specific heat for annealed samples shows a slightly decreased T_c and an increased Θ_D but only small changes of the electronic contribution. To our knowledge a-Cu_xSn_{100-x} and a-Au_xSn_{100-x} films are homogeneous and therefore electronic contributions to the specific heat due to normal-conducting regions below T_c can be excluded.

For contributions of the Zeeman splitting and quadrupole interaction it is expected that $C \propto T^{-2}$; however, we found no indication for this temperature dependence. Estimations for the Zeeman contributions [34] showed that they could be of the same magnitude as C_{LEE} for the worst-case scenario (lowest temperature and highest field). The quadrupole contribution [17, 35] at the lowest temperature could reach about 20% of C_{LEE}. In both cases their contributions would level off with increasing temperature.

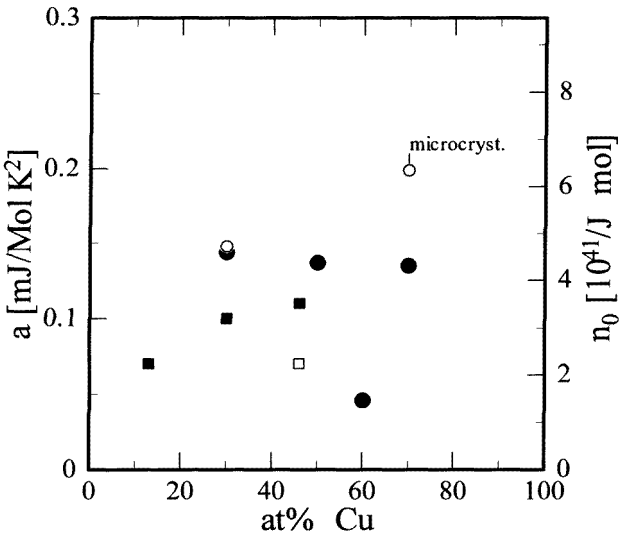

Figure 6. Concentration dependences of the parameter a characterizing the LEE for a-Cu_xSn_{100-x}. The right-hand axis rescales a according to equation (5) to give the density of states n_0 of the LEE. Data from this investigation: as quenched (●) and as annealed (○). Data given by Hofacker *et al* [36]: as quenched (■) and as annealed (□).

4.1. Vibrational contributions to the specific heat

From the arguments just mentioned we conclude that the term of the specific heat proportional to T in the superconducting state is exclusively due to LEE. Figure 6 shows the concentration dependence of the parameter a and of the density of states n_0 of the LEE calculated from equation (5). These values are somewhat larger than the data of [36] measured with a heat pulse method. Probably the small difference is caused by differences

in the sample preparation. The values of n_0 of a-Cu_xSn_{100-x} are of the same order of magnitude as the values for other metallic glasses [37].

We are not sure whether the minimum value of n_0 at $x = 60$ at.% Cu is significant. It may be worth mentioning that at the same concentration $D(E_F)$ also shows a minimum as depicted in figure 10, later. The correlation between the electronic and the structural properties of amorphous metals like a-Cu_xSn_{100-x} was discussed intensively in connection with the concept of AHR phases within the last decade [1, 3, 4, 7]. Because this concept demonstrates successfully the connections between the electronic system and the structure of the alloys it would not be surprising if the LEE and the electronic system were also correlated. Further measurements are certainly necessary to prove whether such a correlation does exist or not.

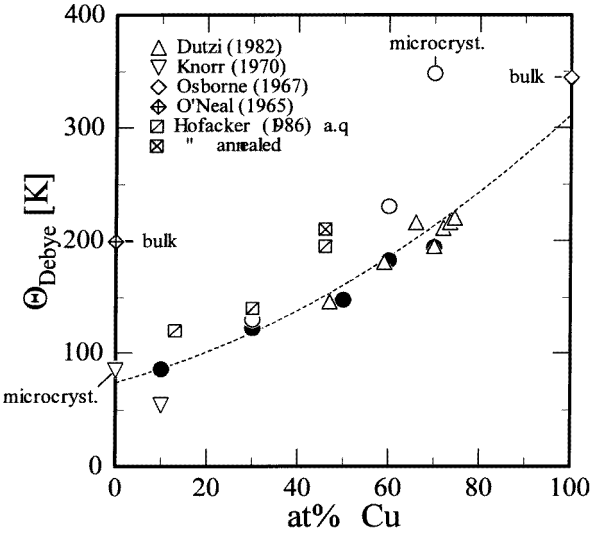

Figure 7. Concentration dependences of the Debye temperature Θ_D of a-Cu_xSn_{100-x} as quenched (●) and as annealed (○). The data are from the literature [6, 36, 48, 49].

The phonon part $C_L(T)$ is described by the two parameters β and δ in our analysis. Figure 7 shows the concentration dependence of the Debye temperature Θ_D calculated from the parameter β and values taken from literature. Θ_D increases with increasing copper concentration and follows roughly an interpolation between the pure elements at a lower level. From electron diffraction measurements it is known that the nearest-neighbour distances decrease with increasing x up to $x = 50$ at.% Cu and remain nearly constant at higher Cu concentrations whereas the number density is continuously increasing [15]. This tendency was explained by an increasing chemical interaction. The fact that annealing the samples increases Θ_D may be explained by changes in the nearest-neighbour ordering.

In figure 8 the parameter δ is shown as a function of the Cu concentration. A correlation between δ and Θ_D was found for crystalline metals [38]. de Launy was able to describe this correlation by a central-force model valid for isotropic metals with fcc or bcc structure [39]. He found

$$\lg \delta = -5 \lg \Theta_D + A. \tag{9}$$

Yamamoto *et al* derived the same dependence from a model for a-Fe [40]. The dashed curve

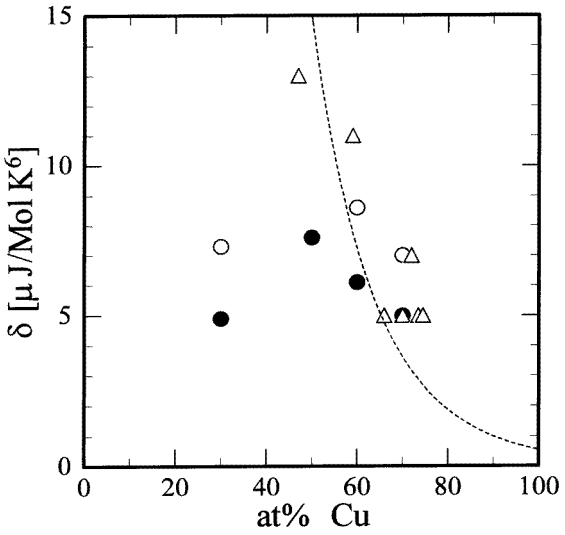

Figure 8. Concentration dependences of the parameter δ of a-Cu_xSn_{100-x} as quenched (●) and as annealed (○), plus data (△) taken from [6].

was calculated using $\Theta_D(x)$ from the specific heat data (dashed line in figure 7) according to equation (9). The best fit was achieved using $A = 7.4$ instead of $A = 6.2$ found for crystalline samples [39, 40]. The strong increase of δ with decreasing $\Theta_D(x)$ is connected to the decrease of the number density [38]. The large deviations from this simple model for $x < 50$ are probably due to the changes of the nearest-neighbour distance which are known from electron diffraction experiments [15].

4.2. Electronic contributions to the specific heat

As already mentioned, the electron–phonon interaction in amorphous metals enhances strongly the density of states at E_F [17–19, 25]. The enhanced density of states $D^\star(E_F)$ is directly proportional to the bare density of states $D(E_F)$ according to equation (2). For the comparison with the FEM we need $D(E_F)$ and therefore the knowledge of the electron–phonon coupling constant λ. The parameter λ was calculated according to the McMillan equation [41]:

$$\lambda = \frac{1.04 + \mu^* \ln(\Theta_D/1.45T_c)}{(1 - 0.62\mu^*)\ln(\Theta_D/1.45T_c) + 1.04} \tag{10}$$

taking the data for T_c and Θ_D from our measurements and assuming as usual $\mu^\star = 0.1$ for the effective Coulomb interaction [25, 41].

The results of this calculation are shown in figure 9 for the as-quenched and the annealed state. Data from the literature are added. It is interesting to note that the λ-values taken from tunnelling measurements are in most cases higher than the values determined by specific heat data with the help of the McMillan equation [42]. A modified version of the McMillan equation which takes into account the amorphous structure yields values for λ about 20% higher than the original equation [43].

The concentration dependence of $D^\star(E_F)$ is shown in the upper part of figure 10. $D^\star(E_F)$ calculated from our critical field measurements is found to be always larger than the results of the specific heat measurements. Moreover the interpolated specific heat data show a pronounced dip at $x = 60$ at.% Cu which is not seen in the values derived from

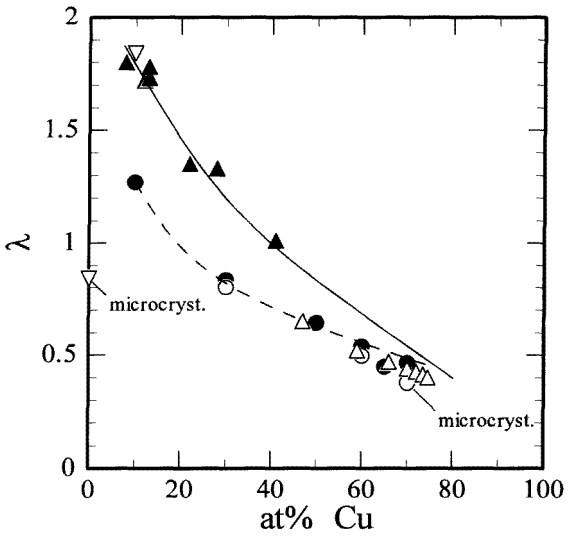

Figure 9. Concentration dependences of the electron–phonon coupling constant λ of a-Cu_xSn_{100-x} calculated from specific heat data using equation (10): as quenched (●) and as annealed (○), and taken from [6] (△). The other symbols show results from tunnelling experiments [18, 19]. The lines show the interpolations for $\lambda(x)$ used for the calculation of $D(E_F)$.

critical field measurements.

Our data calculated from specific heat measurements agree quite well with those of Dutzi and Buckel [6] although they could not measure C_e^n below T_c. They agree also quite well with those values Häußler found from UPS measurements [4] while his critical field measurements [44] give values of $D^\star(E_F)$ even slightly larger than ours.

In contrast to $D^\star(E_F)$ all of the values of $D(E_F)$, shown in the lower part of figure 10, are lower than those calculated according to the FEM (full line). They are calculated using the λ-values of the tunnelling experiments (the solid line in figure 9). In order to show the influence of the uncertainty of λ, we also calculated $D(E_F)$ using the λ-values evaluated from the McMillan equation (the dashed line in figure 9). In both cases the deviation of $D(E_F)$ from the FEM clearly increases with increasing copper content corresponding to the decreasing conduction electron concentration Z. Additionally $D(E_F)$ shows a dip at $x = 60$ at.% Cu. This is in contrast to the somewhat larger values of $D(E_F)$ calculated from critical field measurements. Similar discrepancies are reported in the literature. In the case of disordered Zr–Cu alloys, $D^\star(E_F)$ determined by critical field measurements is 5–10% higher than those values taken from specific heat measurements [45]. The transition to the superconducting state in a perpendicular field observed by resistance measurements can be influenced by many processes, like e.g. flux motions [21], fluctuations [46], inhomogeneities of the sample which are comparable in size to the coherence length [47], strong coupling [21, 24], and localization effects [45]. Because it is difficult to estimate the different contributions of these effects to $(dB_{c2}/dT)\big|_{T=T_c}$ which is proportional to $D^\star(E_F)$ (equation (1)), we prefer to rely on the specific heat measurements for the determination of $D^\star(E_F)$.

We believe that the strong decrease of $D(E_F)$ with increasing x relative to the FEM is caused by the interplay between the electronic and the ionic system. According to the

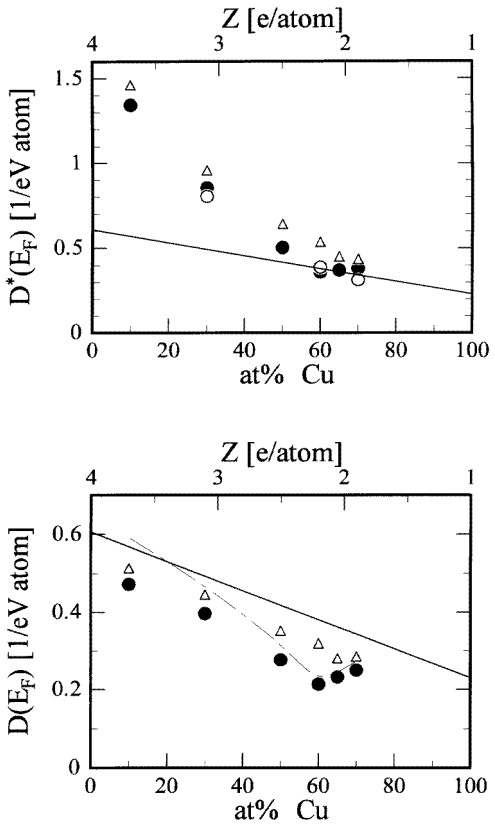

Figure 10. Concentration dependences of the electronic density of states at E_F of a-Cu_xSn_{100-x}. Upper part: $D^{\star}(E_F)$; lower part: $D(E_F)$. The specific heat data are shown for as-quenched (●) and as-annealed (○) samples. Also shown are values calculated from critical field data (◊). The values of $D(E_F)$ (●) were calculated using the interpolation (——) in figure 9 of $\lambda(x)$. The dashed line corresponds to $\lambda(x)$ derived from equation (10) (the dashed line in figure 9). The full line gives $D(E_F)$ calculated according to the free-electron model. Z gives the concentration of the conduction electrons obtained assuming that Cu provides one electron per atom and Sn four electrons per atom.

Nagel–Tauc criterion this interplay should be strongest for amorphous alloys if the diameter of the Fermi sphere $2k_F$ is equal to a main peak position k_P in the structure factor. In a-Cu_xSn_{100-x} this is the case for about $x = 70$ at.% Cu [4]. In many amorphous alloys similar to a-Cu_xSn_{100-x}, UPS measurements showed a decrease in the density of states towards E_F as a function of x which is strongest for alloys with $2k_F = k_P$. Recently Kroha *et al* [3] calculated the static electronic response $\chi(0, q)$ in disordered metals. They found that the quantum interference between the Coulomb interaction and impurity scattering causes a logarithmic divergence of $\chi(0, q)$ at the Fermi surface. This causes a phase shift of the Friedel oscillations as well as an enhancement of their amplitude which is most pronounced at $k_P = 2k_F$. This results are in agreement with experiments [4] and may explain the stability of AHR alloys against crystallization. In addition they found that the minimum in the DOS is most pronounced for slightly higher electron concentration Z than predicted by the simple Nagel–Tauc criterion which yields $Z = 1.8$, corresponding to $x = 70$ at.% Cu. This is in

excellent agreement with the dip of $D(E_F)$ at $x = 70$ at.% Cu (figure 10) resulting from the analysis of our specific heat data.

In conclusion, we take the increasing deviation from the FEM with increasing x which reflects the increasing minimum in the DOS observed in UPS measurements as well as the dip in the concentration dependence of $D(E_F)$ of a-Cu_xSn_{100-x} as additional support for the concept of AHR alloys.

4.3. A remark on former results on a-Au_xSn_{100-x}

From previous measurements of the specific heat and the critical field of a-Au_xSn_{100-x} Rieger and one of us (FB) found $D(E_F)$ in agreement with the FEM prediction [9]. This unexpected result which was clearly in contradiction to UPS measurements [5] stimulated the present investigation on a-Cu_xSn_{100-x} and a-$Au_{70}Sn_{30}$ to scrutinize the earlier measurements.

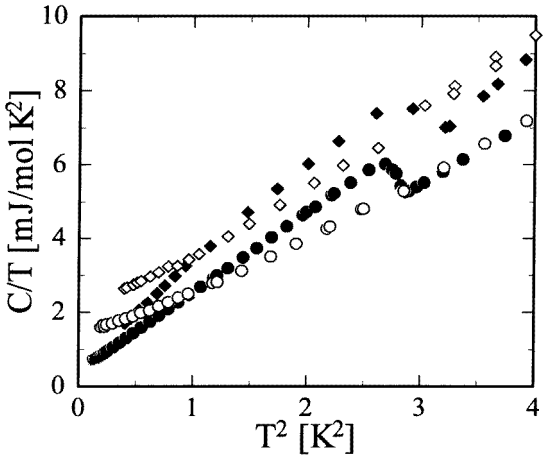

Figure 11. Results for the specific heat of a-$Au_{70}Sn_{30}$; circles, this work; diamonds, Rieger and Baumann [9]; full symbols, $B = 0$; open symbols, $B > B_{c2}$.

In figure 11 results of our specific heat measurements are shown for an a-$Au_{70}Sn_{30}$ alloy. For this composition UPS measurements showed the strongest deviations of $D(E_F)$ from the FEM-like behaviour. For comparison the old data for an alloy with the same composition are also shown. Below 2 K the old data are about 25% higher and at higher temperatures about 15% higher than data taken during this investigation. This discrepancy is independent of the applied magnetic field. In addition the specific heat above T_c was magnetic field dependent in the old experiment, $C(B = 0) \neq C(B > B_{c2})$ in contradiction to the thermodynamic condition of equal entropy at T_c, which is a clear indication of the lower accuracy of this investigation.

As far as we could reconstruct, possible differences in the quality of the two samples shown in figure 11 are negligible. Further, we suppose that the large deviation is not caused by an error in determining the mass of the sample. We could not detect any specific error in the old measurements but we believe that they are systematically wrong eventually because of errors in the heater resistance, in the data acquisition or in its analysis. According to our recent investigation, $D(E_F)$ for a-$Au_{70}Sn_{30}$ is about 20% lower than the value calculated on the basis of the FEM in agreement with UPS measurements which found a pronounced minimum of the DOS in this concentration range [5].

5. Summary

We measured the specific heat of a-Cu_xSn_{100-x} for $B = 0$ and $B > B_{c2}$. This allows the separation of the electronic contribution from the contribution of the low-energy excitations. By fitting these values to theory the contributions of electrons, structural low-energy excitations and lattice vibrations can be calculated quantitatively and consistently in the normal as well as in the superconducting state. The contribution of lattice vibrations can be described by the harmonic lattice theory. We show that the linear contribution in the superconducting state can be explained by the standard tunnelling model of structural low-energy excitations. This contribution is comparable to values found for other glasses. The electronic contribution in the superconducting state can be described within BCS theory in the weak-coupling limit. For the samples with high tin content this description is no longer valid; the description with a BCS expression modified for strong coupling yields values for the energy gap which are in agreement with results from tunnelling experiments. From the electronic contribution in the normal state the density of states at the Fermi level was determined. With the electron–phonon coupling constant known from tunnelling experiments we calculated the bare-band-structure density of states. It shows a minimum compared to the free-electron model in agreement with results from UPS measurements and theoretical predictions. The observed dip of the density of states at 60 at.% Cu can be explained on the basis of a recently published theory, calculating quantum corrections to the static electronic response which cause a phase shift of the Friedel oscillations as well as an enhancement of their amplitude. This enhancement of the Friedel oscillations explains the stability of amorphous Hume-Rothery alloys against crystallization. Values of the density of states calculated from critical field measurements are somewhat higher but still well below the free-electron model values. In addition we measured the specific heat of a-$Au_{70}Sn_{30}$. In agreement, with UPS measurements but in contradiction to former specific heat measurements of Rieger and one of us (FB), we found the density of states to be well below the free-electron model results for this sample.

Acknowledgments

We are grateful to P Häußler, J Kroha, H von Löhneysen, P Rieger, and H Wühl for valuable discussions. This work was supported partially by the *Graduiertenförderung des Landes Baden-Württemberg*.

References

[1] Nagel S R and Tauc J 1975 *Phys. Rev. Lett.* **35** 380
[2] Beck H and Oberle R 1980 *J. Physique Coll.* **41** C8 289
[3] Kroha J, Huck A and Kopp T 1995 *Phys. Rev. Lett.* **75** 4278
[4] Häußler P 1992 *Phys. Rep.* **222** 65
[5] Häußler P, Baumann F, Krieg J, Indlekofer J, Oelhafen P and Güntherodt H-J 1983 *Phys. Rev. Lett.* **51** 714
[6] Dutzi J and Buckel W 1984 *Z. Phys.* B **55** 99
[7] Hafner J, Jaswal S S, Tegze M, Pflugi A, Krieg J, Oelhafen P and Güntherodt H J 1988 *J. Phys. F: Met. Phys.* **18** 2583
[8] van den Berg R, Grodney S, Kästner J and von Löhneysen H 1983 *Solid State Commun.* **47** 137
Mizutani U 1983 *Prog. Mater. Sci.* **28** 97
[9] Rieger P and Baumann F 1991 *J. Phys.: Condens. Matter* **3** 2309
[10] Velichkov I V 1992 *Cryogenics* **32** 285
[11] Sohn M 1995 *Thesis* University of Karlsruhe, 1994 (Aachen: Shaker)
[12] Menges H and von Löhneysen H 1991 *J. Low Temp. Phys.* **84** 237

[13] Phillips N E 1964 *Phys. Rev.* **134** A385
[14] Buckel W and Hilsch R 1952 *Z. Phys.* **131** 420; 1954 *Z. Phys.* **138** 109
Buckel W 1954 *Z. Phys.* **138** 136
[15] Leitz H 1980 *Z. Phys.* B **40** 65
[16] Fortmann J and Buckel W 1961 *Z. Phys.* **162** 93
Korn D, Pfeifle H and Zibold G 1974 *Z. Phys.* **270** 195
Reichel G 1984 *Diploma Thesis* University of Karlsruhe
Lauinger C 1990 *Diploma Thesis* University of Karlsruhe
[17] Bolz J and Pobell F 1975 *Z. Phys.* B **20** 95
[18] Knorr K and Barth N 1970 *Solid State Commun.* **8** 1085
[19] Watson P W III and Naugle D G 1995 *Phys. Rev.* B **51** 685
[20] Köpke R and Bergmann G 1971 *Z. Phys.* **242** 31
[21] Bergmann G 1973 *Phys. Rev.* B **7** 4850
[22] Helfand E and Werthamer N R 1966 *Phys. Rev.* **147** 288, 295
[23] Bergmann G 1976 *Phys. Rep.* **27** 159
[24] Rainer D and Bergmann G 1973 *J. Low Temp. Phys.* **14** 501
[25] Grimvall G 1981 *The Electron–Phonon Interaction in Metals* (Amsterdam: North-Holland)
[26] Sullivan P F and Seidel G 1968 *Phys. Rev.* **173** 679
[27] Mühlschlegel B 1959 *Z. Phys.* **155** 313
[28] 1980 *Amorphous Solids: Low Temperature Properties (Springer Topics in Current Physics 24)* ed W A Phillips (Heidelberg: Springer)
[29] Phillips N E 1971 *CRC Crit. Rev. Solid State Sci.* **2** 467
[30] Bardeen J and Schrieffer J R 1961 *Progress in Low Temperature Physics* vol 3, ed C J Gorter, ch VI (Amsterdam: North-Holland)
[31] Zougmoré F, Lasjaunias J C and Béthoux O 1989 *J. Physique* **50** 1241
Lasjaunias J C and Zougmoré F 1989 *Solid State Commun.* **71** 579
Zougmoré F, Lasjaunias J C and Béthoux O 1988 *Proc. ILL Workshop on Dynamics of Disordered Materials (Grenoble, 1988)* ed D Richter *et al* (Berlin: Springer)
[32] Rühl W 1954 *Z. Phys.* **138** 121
[33] Samwer K and von Löhneysen H 1982 *Phys. Rev.* B **26** 107
[34] Freeman A J and Watson R E 1965 *Magnetism* vol IIa, ed T Rado and H Suhl (London: Academic)
Handbook of Chemistry and Physics 1982 ed R C Weast and M J Astle (Boca Raton, FL: Chemical Rubber Company Press) p E-69
[35] Lasjaunias J C, Ravex A and Thoulouze D 1979 *J. Phys. F: Met. Phys.* **9** 803
[36] Hofacker M, Sander W, Sürgers C and von Löhneysen H 1987 *Japan. J. Appl. Phys. Suppl.* 3 **26** 737
[37] Sürgers C and von Löhneysen H 1988 *Z. Phys.* B **70** 361
Sürgers C, von Löhneysen H and Schultz L 1989 *Phys. Rev.* B **40** 8787
[38] Mizutani U and Massalski T B 1980 *J. Phys. F: Met. Phys.* **10** 1093
[39] de Launy J 1956 *Solid State Physics* vol 2, ed F Seitz and D Turnbull (New York: Academic) p 220
[40] Yamamoto R, Haga K, Mihara T and Doyama M 1980 *J. Phys. F: Met. Phys.* **10** 1389
[41] McMillan W L 1968 *Phys. Rev.* **167** 331
[42] von Löhneysen H 1993 *Rapidly Solidified Alloys* ed H H Liebermann (New York: Dekker) p 461
[43] Garland J W, Bennemann K H and Mueller F M 1968 *Phys. Rev. Lett.* **21** 1315
[44] Häußler P 1981 unpublished results
[45] Nordström A, Dahlborg U and Rapp 1993 *Phys. Rev.* B **48** 12 866
[46] Aslamazov L G and Larkin A I 1968 *Phys. Lett.* **26A** 238
Ferrell R A 1969 *J. Low Temp. Phys.* **1** 241
Glover R E 1967 *Phys. Lett.* **25A** 542
[47] Zwicknagel G E and Wilkins J W 1984 *Phys. Rev. Lett.* **53** 1276
[48] O'Neal H R and Phillips N E 1965 *Phys. Rev.* **137** A748
[49] Osborne D W, Flotow H E and Schreiner F 1967 *Rev. Sci. Instrum.* **38** 159